



Research paper

A Novel Method of FACTS-POD Design to More Enhancement of Inter-area Mode Damping in a Multi-machine Power System

B. Ehsan Maleki^{1,*}, H. Beiranvand²

¹Shahid Rajaei Teacher Training university, Tehran, Iran.

²Lorestan University, Khorram Abad, Iran.

Article Info

Article History:

Received 09 February 2017

Revised 10 June 2017

Accepted 11 November 2017

Keywords:

FACTS-POD

GMDC

Probabilistic sensitivity indices

*Corresponding Author's Email
Address:

b.ehsanmaleki@sru.ac.ir

Extended Abstract

Background and Objectives: In this paper, a non-typical design method of flexible AC transmission systems power oscillation damping (FACTS-POD) controller is proposed to increase the efficiency of these devices. In all of the introduced FACTS-POD devices (taking IPFC-POD as an example), the supplementary controller is designed based upon a conventional approach (i.e., based on optimization algorithms) and using a different method can be useful.

Methods: In this paper, the graduated modal decomposition control (GMDC) is utilized as a specific strategy for POD controller design. Moreover, the dynamic model of the multi-machine power system with the presence of IPFC devices has been developed.

Results: The obtained model is nonlinear; however, it is linearized around the operating point to design the controllers. The overall paper's structure is based upon the two scenarios, in the first of which conventional method for IPFC-POD design has been analyzed there upon the result compared with the introduced method in the second scenario. Finally, to ascertain responsive of the designed controller to load changes and stability of the system, the probabilistic sensitivity indices (PSIs) are investigated over a large set of operating conditions. As a verification, the time-domain simulations on a 10-machine power system emphasize the analysis of dynamic results and their information under the considered conditions.

Conclusion: In general, the specific purpose of this paper is to enhance of the dynamic stability of concerned inter-area modes. The proposed method, especially using GRSA, offers better stability characteristics than the results of previous methods.

Introduction

Nowadays, insufficient access to resources due to the strict environmental constraints and deregulation of power utilities have caused delays in the construction of both generation facilities and new transmission lines. These limited factors consider the need to pay attention to the modern concepts and workout of connected power systems [1], [2]. One of the most powerful tools to cope with mentioned problems is power system

stabilizer (PSS) which its effectiveness in reducing the inter-area oscillations is widely accepted and verified in practice.

In our previous work [5], a two-stage approach to design wide-area power system stabilizer (WAPSS) that simultaneously uses the advantages of optimization algorithms and GMDC method is presented. Also, the performance of general relativity search algorithm (GRSA) was considered in solving optimization problems. In addition, there is another emerging technology known

a FACTS that can be effective in counteracting fluctuations in the power system [2], [6]-[10].

This technology, launched by EPRI in the 1980s, is a revolution in the development of electronics-based devices, which include some of the recent works such as Bhowmick *et al.* [9] proposed an advanced IPFC model for solving the newton–raphson load flow (NRLF) analysis during interline power flow controller (IPFC) modeling. So, wherein an existing power system including IPFC is transformed into an augmented equivalent network without any IPFC. Guo *et al.* [10], proposed a unified power flow controller (UPFC) control method to enhance the small-signal stability characteristics of a power system. The introduced scheme is also effective under the conditions of multi-mode oscillations. The simultaneous adjustment of FACTS and conventional power system stabilizer (CPSS) controllers in multi-machine power systems is a very important problem, which is presented in some recent research in [11]-[12]. Bian *et al.* [11] used the probabilistic theory to adjust the coordination of PSSs and static var compensator (SVC) controllers. Actually, a coordinated set of controller’s parameters is obtained with an optimization process based on a probabilistic objective function. Shayeghi *et al.* [12], developed a simultaneous coordinated design procedure of the thyristor controlled series capacitor (TCSC) and PSS controllers in a multi-machine power system. Coordinated design of controllers converted to an optimization problem in which the defined objective function solved via a particle swarm optimization (PSO) technique. Now, many FACTS manufacture include supplementary damping controller (SDC) denominated as POD to more enhance of the rate of oscillation damping in the interconnected power system. Considering the impressive efficiency of these devices, it has achieved a growing interest [13]-[14]. Visakhan *et al.* [13], evaluated the performance of several FACTS-POD devices such as SVC, static synchronous compensator (STATCOM), TCSC and static synchronous series compensator (SSSC) with POD with respect to system loss reduction and also overall stability enhancement capability. Makkar *et al.* [14] investigated the simultaneous coordination performance of UPFC-POD and PSS to control with the low-frequency oscillations (LFOs) and deal to disturbances occurred in the power system. So far, numerous attempts have been made with employ meta-heuristic algorithms (MHAs) in different designs of PSSs, which some lately significant efforts are as [15]-[16] Khaleghi *et al.* [15], presented a modified artificial immune network (MAINet) algorithm and a multi-objective immune algorithm (MOIA) for multi-objective coordinated tuning of supplementary controllers. Beiranvand *et al.* [16], proposed the global

relativity search (GRS) algorithm, which is a MHA inspired by general relativity theory (GRT). In this method, the particle population is considered to be in an open space from all non-gravitational external fields and moves to a position with minimal action.

This paper presents a new design method for FACTS-POD which particularly is based on a GMDC-based approach of designing SDCs. It can be inferred from previous researches that CPSS is often used as a POD supplementary controller in FACTS devices. Now, in this paper, the following method of FACTS-POD design with using a specific method of designing POD is proposed for further improvement in the inter-area mode’s damping.

- Considering a two-stage PSS design method dealing with tune of POD and PSSs used in the test system.
- Coordinated tuning of FACTS-POD and PSSs in the test system.

Increasing the small-signal stability with a predetermined POD controller can provide a situation that exceeds the positive effect of additional damping and reduces the detrimental effect of the weak inter-area mode’s damping in the overall dynamic stability.

The organization of the paper is as follows: The second section introduces methods of design of power system and controller devices. The third section deals with problem statement and review of the applied techniques. The model of the power system, as well as the results of frequency and time-domain simulations of the IEEE 10-machine (New England) power system, is present in the fourth section; and finally, some conclusions are presented in the last section.

Power System Equipment's Modelling

A. Interline Power Flow Controller Device Model

The activation form of FACTS devices in power systems is determined by their classification, which means that they can be used as shunt or series compensation or even angular control of the transmission line. The block diagram of considered IPFC device is shown in Figure 1. This device is composed of two gate turn-off thyristor (GTO)-based VSCs inverter which each of them provides a series compensation for the related line. These VSCs are connected through a direct current (DC) link which is responsible for transmitted active power, and their output is coupled to transmission lines through coupler series transformers (CSTs).

For modeling the IPFC device as it obvious in Figure 2, two coupler transformer, a branch of inverter voltage source and DC link are considered.

The mathematical model of both VSCs for each three-phase is obtained in the rotational framework same as [18], [19] which presented in Equations 1-8. It should

be mentioned that the value of r_{cST} is ignored in this model.

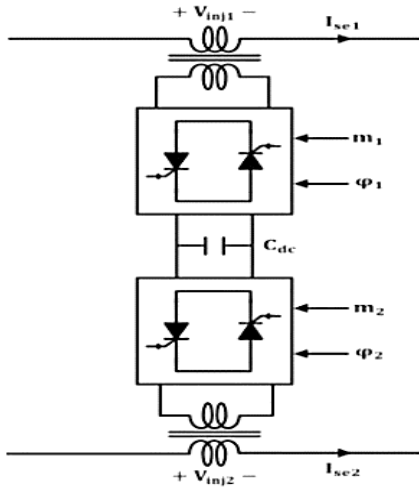


Fig. 1: Block diagram of the IPFC device.

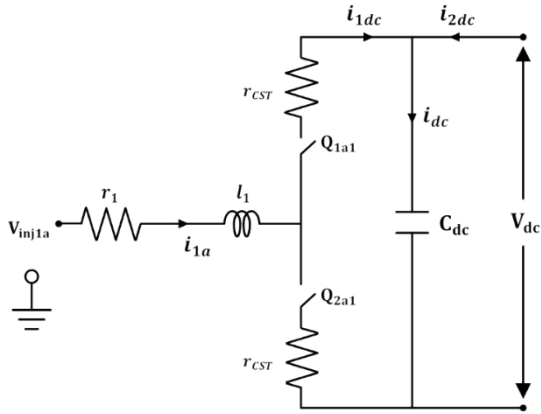


Fig. 2: Single-phase equivalent circuit of VSC with coupler transformer.

$$\begin{bmatrix} V_{inj1d} \\ V_{inj1q} \end{bmatrix} = \begin{bmatrix} 0 & -x_{t1} \\ x_{t1} & 0 \end{bmatrix} \begin{bmatrix} I_{se1d} \\ I_{se1q} \end{bmatrix} + \begin{bmatrix} V_{se1d} \\ V_{se1q} \end{bmatrix} \quad (1)$$

$$\begin{bmatrix} V_{inj2d} \\ V_{inj2q} \end{bmatrix} = \begin{bmatrix} 0 & -x_{t2} \\ x_{t2} & 0 \end{bmatrix} \begin{bmatrix} I_{se2d} \\ I_{se2q} \end{bmatrix} + \begin{bmatrix} V_{se2d} \\ V_{se2q} \end{bmatrix} \quad (2)$$

$$\frac{dV_{dc}}{dt} = \frac{3}{2C_{dc}V_{dc}} \operatorname{Re} \left\{ \sum_{k=1}^2 V_{sek} I_{sek}^* \right\} \quad (3)$$

$$C_{dc}V_{dc} \frac{dV_{dc}}{dt} = \frac{3}{2} \operatorname{Re} \left\{ \sum_{k=1}^2 V_{sek} I_{sek}^* \right\} = -\frac{3}{2} P_{IPFC} \quad (4)$$

$$\tilde{V}_{sek} = \frac{l_k V_{dc}}{2} e^{j\gamma_k} \quad (5)$$

$$\tilde{V}_{sek} = h_k \tilde{V}_{SEk} e^{j(\gamma_k)} = h_k V_{SEk} e^{j(\gamma_k + \psi_k)} \quad (6)$$

$$V_{sek} = V_{sekd} + jV_{sekq} \quad (7)$$

$$I_{sek} = I_{sekd} + jI_{sekq} \quad (8)$$

The series voltage source (V_{sek}), which is formulated as Equation 6, is controllable in magnitude and angle by the parameters h_k and ψ_k , respectively.

B. Supplementary Damping Controllers of PSS and POD

In order to increment of LFOs damping, FACTS devices should be equipped with POD controller. The structure of the PSS and POD controller are same to each other, which is a commonly used lead-lag controller. Moreover, despite the same structure for these devices, the operation mode and the output signals of each controller are distinct. The completion of the PSS and POD to the control loop of synchronous generators and FACTS devices (in this work, the IPFC device) respectively are depicted in the Figure 3, [20]. The considered damping controller structure is denoted as follows:

$$G_{PSSi}(s) = K_i^{PSS} \frac{T_w s}{(1 + sT_w)} \frac{(1 + sT_{1i})(1 + sT_{3i})}{(1 + sT_{2i})(1 + sT_{4i})} \quad (9)$$

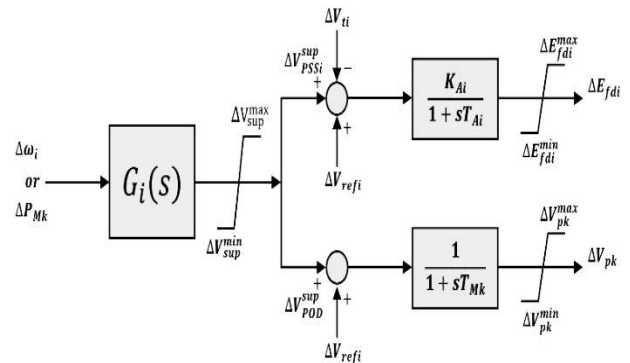


Fig. 3: Overall interconnection of PSS and POD controller with considered excitation system and primary converter of the IPFC.

C. Dynamic Model of the Power System Equipped With The IPFC Device

This section presents an integrated dynamic model of power system with the IPFC device. As shown in Figure 4, this model constructed based on the system admittance matrix and also differential algebraic equations (DAEs) of generators, loads and IPFC device. In the obtained model, each of VSCs is considered as a new bus, and the lines network is depicted with Y_{new} as equivalent admittance matrix.

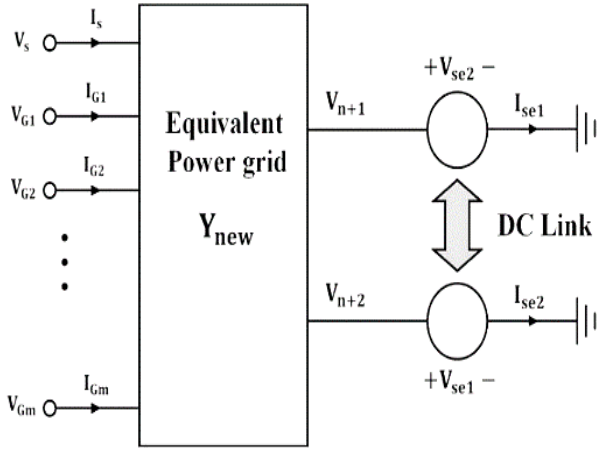


Fig. 4: Dynamic model of the IPFC device in the power system.

Algebraic equations include of stator, network and IPFC equations. For all generators, algebraic generator equations (GAEs) can be written in the form of a compact matrix:

$$\begin{bmatrix} V_d \\ V_q \end{bmatrix} = \begin{bmatrix} 0 & X_q \\ -X'_d & 0 \end{bmatrix} \begin{bmatrix} I_d \\ I_q \end{bmatrix} + \begin{bmatrix} 0 \\ E'_q \end{bmatrix} \quad (10)$$

In this paper, the dynamical modeling of an n-bus system with one infinite type (S), m generator types (G) and n-m-1 load types buses are accompanied by an advanced IPFC model which is based on [9]. In this model, the SVC number of IPFC determines the number of system buses and the new admittance matrix is obtained with a very little change over the old admittance matrix. Moreover, the admittance matrix of the system with the presence of IPFC is symmetrical and is constant during the dynamic and transient studies. This model has been extensively reviewed and validated in the simulation section. Network equations of the system in the presence of IPFC can be written as follow:

$$I_{BUS} = Y_{BUS} V_{BUS} \quad (11)$$

By absorbing the loads of the network in type of constant impedance, the new admittance matrix is given as below:

$$I_{new} = Y_{new} V_{new} \quad (12)$$

$$V_{new} = [V_S \ V_G \ V_{IP}]^T \quad (13)$$

$$I_{new} = [I_S \ I_G \ I_{IP}]^T \quad (14)$$

Problem Statement and Review of the Applied Techniques

A. Problem Statement

The linearized set of algebraic equations independent of the damping controller's structure, which cover the

behavior of the power system at a point of equilibrium, can generally be as follows:

$$\frac{d\Delta x}{dt} = A\Delta x + B\Delta u \quad A \in R^{n \times n} \quad ; B \in R^{n \times 1} \quad (15)$$

$$\Delta y = C\Delta x + D\Delta u \quad C \in R^{1 \times n} \quad ; D \in R^{n \times 1} \quad (16)$$

The vector of state variables is $x = [\delta, \omega, E'_q, E_{fd}]$

A.1. Define the objective function

To achieve the appropriate dynamic characteristic, the selection of controller parameters with optimization method is achieved by minimizing the damping ratio objective function (F_1), whose convergence region is shown in Figure 5 [22]. The objective function is calculated as follows:

$$\text{Min } F_1 = \sum_{y=1}^{n_y} \left(\xi_0 - \min_{1 \leq q \leq n_q} \xi_q \right)_y \quad (17)$$

Subject to:

$$\begin{cases} 0.01 \leq K_i^{PSS} \leq 50 \\ 0.01 \leq T_{1i} \leq 1 \\ 0.02 \leq T_{2i} \leq 1 \\ 0.01 \leq T_{3i} \leq 1 \\ 0.02 \leq T_{4i} \leq 1 \end{cases} \quad (18)$$

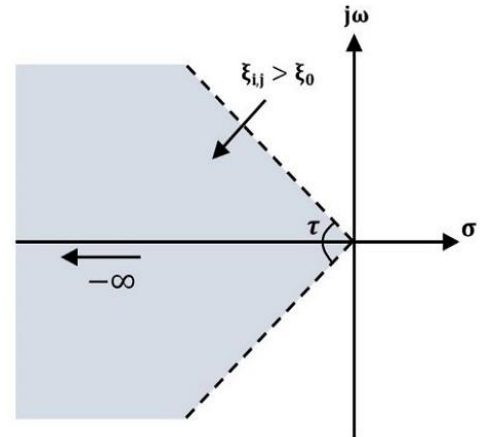


Fig. 5: Fan-shaped region with the tip at the origin of damping ratio [14].

A.2. Review of the two-stage design approach of SDCs and probabilistic eigenvalue sensitivity index

With regard to the research on PSS design, it could be concluded that numerous studies have examined one-stage design methods such as MDC and optimization methods. This subsection dealt to review of a two-stage WAPSS design approach that has been presented in our previous work [5]. The general strategy

is in this way that both the properties of the GMDC and the optimization algorithm are used simultaneously. The approach in each stage has been used to design PSS, separately. Nevertheless, both stage of PSS design have a positive impact on each other. The two stage to implement the method are as follows:

Stage 1: Enhancing the local mode's damping with the use of the optimization algorithm (GRSA)

Stage 2: Enhancing the inter-area mode's damping with the use of the GMDC method

In this paper, an approximation of bus loads is made by normal distributions, which average index (μ) is considered as estimated values of each load. The normal distribution is constructed based on (n_l) series loads. With the approximation of bus loads as distributed random variables by normal distribution, an assumption of nodal voltage and the derived eigenvalues to have normal distribution can be reasonable. In the stability measurement of the power system in multi-operating conditions, we must consider the probabilistic distribution of damping factor α and damping ratio ξ . In this study, the effects of damping controller parameter for both α and ξ are shown with probabilistic sensitivity indices (PSIs). For complex eigenvalue $\lambda_k = \alpha_k + j\beta_k$, to achieve the wide extent of stability of the system, a high reliable index of $4\sigma_{\alpha_k}$ have been implemented [24]-[25]. The upper range of this distribution range (α'_k) as an extended damping coefficient can be used to assess the stability of the test system under the wide range of operation.

Similarly, the extended value ξ'_k for the damping ratio of the k^{th} eigenvalue can be defined as (20). The adequate stability of the system is attained under the condition in which $\alpha'_k \leq 0$ and $\xi'_k \geq \xi_c$ ($\xi_c = 0.1$ is considered for the present study).

$$\alpha'_k = \bar{\alpha}_k + 4\sigma_{\alpha_k} \leq 0 \quad (19)$$

$$\xi'_k = \bar{\xi}_k - 4\sigma_{\xi_k} \geq \xi_c \quad (20)$$

The standardized expectation index that can be obtained by rewriting the inequality of (19) and (20), respectively, as equations of (21) and (22), can also be used to measure the stability criteria.

$$\alpha_k^* = -\bar{\alpha}_k / \sigma_{\alpha_k} \geq 4 \quad (21)$$

$$\xi_k^* = (\bar{\xi}_k - \xi_c) / \sigma_{\xi_k} \geq 4 \quad (22)$$

Whilst α'_k and ξ'_k only indicate the upper limit of the distribution of stability criteria, the standardized coefficients of α_k^* and ξ_k^* reflect the distribution

probability of $\{\alpha_k < 0\}$ and the degree of stability, respectively. Therefore, stability indicator of (21) and (22) is more suitable for tuning of controller parameter than (19) and (20).

Tests and results

This section addresses the coordinated design of the PSSs and the FACTS-POD device and also evaluates stability test across a multi-machine test system (New England) in the wide range of operating conditions. The single-line diagram of the New England test system which its detailed data are enclosed in [21] is depicted in Figure 6(a). Figure 6(b) shows separated part of the power system which included the IPFC device between two considered fictitious buses. In this diagram, two fictitious buses (FBs), FB_1 and FB_2 , and two tie lines (TLs) of (37- FB_1) and (37- FB_2), are included to perform simulations with the IPFC. This system was equipped with eight PSSs at the generators $G_1, G_2, G_3, G_4, G_5, G_7, G_8$, and G_9 , and an IPFC-POD. The locations of the PSSs in all systems were determined by the participation factors and sensitivity analyses, which indicated the generators that were more involved in the formation of each critical modes.

A. Static Analysis

Overall, due to the complexity of the interconnected power system and presence of various type of instable oscillatory modes, it is necessary to use a systematic approach to select locations of the devices such as FACTS-POD. These locations were determined by technical factors.

In order to investigate critical buses (buses with voltage magnitudes in out of the acceptable limits ($\pm 5\%$ of the nominal value)), we can consider extracted voltage profile which is shown in Figure 6(c). This figure depicts the difference between voltage magnitude of each bus and base value (0.95 p.u). In this way, this profile indicated the buses involved in the low voltage problems as buses 12, 15, 33, 36, and 37 which also justified the installation of the IPFC at this location. The ideal place which chosen for the installation of the IPFC device would be in the TL between buses 10 and 38.

As there is only a line between these buses, it was impractical to install the device on this site; therefore, it was installed between buses 34, 36, and 37. It was expected that the IPFC device would improve the voltage profile at these buses, through the active and reactive power flow control.

B. Dynamic Analysis

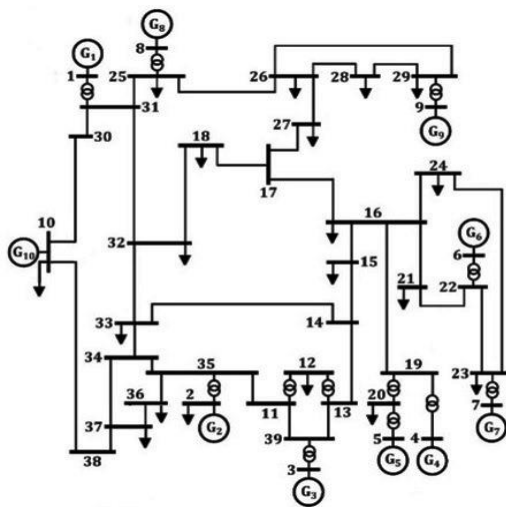
The probabilistic results of the nine oscillatory open-loop eigenvalues of the test system presented in Table 1. The presence of one or more than one modes with the positive real part classified the system as unstable with

the normal distribution of loads. The stable electromechanical modes of the test systems can be separated into two groups: high-frequency and well-damped modes and also low-frequency and poorly-damped modes.

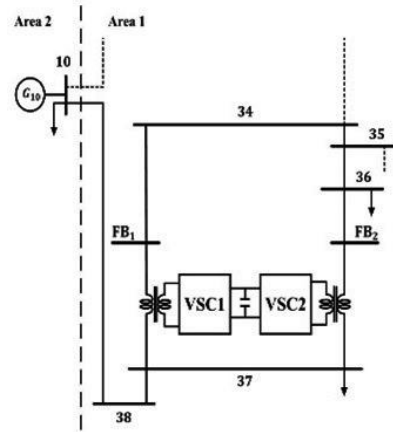
For investigating the margin of system stability, two parameters of α^* and β^* are useful to evaluate. From Table 1, stabilities of the all modes are inadequate: modes 1 to 4 and 5 in spite of positive values of $\bar{\alpha}$ and with the values of α^* greater than 4, have the negative values of β^* .

Between modes 6, 8 and 9, which have negative values of α^* , two modes of 6 and 9 have lower negative values of β^* and are critical modes. The dominant critical modes that have a lower margin of stability, are typed in bold. In order to determine the nature of the critical modes and their associated generators, the sensitivity analysis results are presented in Table 2. The magnitude of the k^{th} element of the modal matrix (m_k) illustrates the significant k^{th} generator's variable (x_k) having large entries in the i^{th} mode of the state matrix. In order to sensitivity analyses, the 26th operating condition between four conditions of 12, 26, 38 and 43 as cases which have the lowest margin of stability is selected (Result of extracted operating conditions from n_l series of loads, and also sensitivity analyses of them because of space-constrained are not shown). From Table 2, it has been observed that the 6th and 9th modes are more affected by the 6th and 5th machines, respectively.

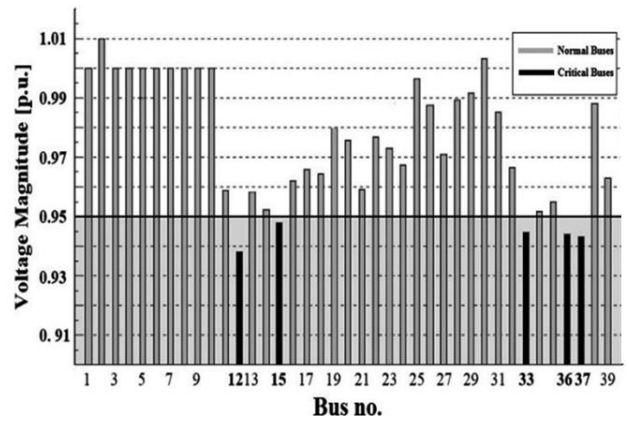
Since the nature of the oscillatory modes are determined based on the swing angle deviation between the specific generator contributed in the i^{th} mode and the other generators, the 9th mode can be classified as inter-area mode, whereas the other concerned oscillatory mode is the local type.



(a)



(b)



(c)

Fig. 6: System diagrams and chart. (a) One-line diagram of the IEEE 10-machine test system, (b) Separated part of the power system with the IPFC device, (c) Extracted voltage profile of the test system.

To enhance overall system damping, both type of SDCs such as PSSs and POD are required. The important step is to choose the best way to use these two types of damping controllers.

The next section overviews the proposed strategy for SDCs design, and also in the obtained results of two scenarios are analyzed.

C. Proposed Strategy to Sdcs (PSS and IPFC-POD) Design

The tests for the considered system were performed considering two different scenarios. In the defined scenarios, methodology of SDCs design is the significant subject, which in the first one, the effectiveness of IPFC-POD with predesigned POD (conventional method with optimization algorithms) illustrated and in the second one, the result of that compared with the proposed method. The detailed description of each scenario is as follows.

Table 1: Open-loop eigenvalues of electromechanical modes

No.	Eigenvalues			Statistical parameters			
	$\bar{\alpha}$	$\bar{\beta}$	σ_{α}	α^*	$\bar{\xi}$	σ_{ξ}	ξ^*
1	-0.16915	8.34593	0.001919	88.1449	0.020263	0.000237	-336.4430
2	-0.14694	8.27169	0.001303	112.7705	0.017761	0.000152	-541.0461
3	-0.20241	8.10227	0.002191	92.3825	0.024974	0.000256	-293.0703
4	-0.1292	7.21493	0.007893	16.3689	0.017906	0.001102	-74.4955
5	0.05674	6.86048	0.008337	-6.8058	-0.00827	0.001213	-89.2580
6	0.28001	5.84364	0.013975	-20.0367	-0.04786	0.00234	-63.1341
7	-0.00364	6.37426	0.087023	0.0418	0.00026	0.014078	-7.0847
8	0.11753	6.12867	0.086029	-1.3662	-0.01944	0.013929	-8.5749
9	0.16242	3.02977	0.020987	-7.7393	-0.05370	0.00811	-18.9426

Table 2: Mode's impact of variables (mode shapes)

Generator	Mode shape of concerned modes	
	6 th mode (λ_6)	9 th mode (λ_9)
G₁	0.0543∠114.9818	0.1655∠-27.0392
G₂	0.0860∠-27.835	0.2021∠-35.9654
G₃	0.0569∠-24.937	0.1946∠-27.4196
G₄	0.0171∠105.4120	0.2267∠-13.6043
G₅	0.1658∠8.43352	0.2876∠149.6623
G₆	0.212∠-175.380	0.2342∠-27.2396
G₇	0.1874∠-178.6708	0.2147∠-22.9229
G₈	0.0384∠112.4511	0.1695∠-26.9216
G₉	0.0757∠35.78005	0.1910∠-21.9517
G₁₀	0.0008∠-80.300	0.1508∠163.0182

C.1. First scenario

In this subsection, as previously mentioned, the goal is to adjust the coordination of SDCs with a powerful algorithm for optimization, and thus, a desired control over the test system is introduced.

The simulation results of this test are done by GRSA. Considering the sensitivity analysis results, the concerned inter-area mode (9th mode) more influenced by the G_5 , which oscillates versus the predominant generator group of $G_{1,3,6-9}$. The feedback combination input signal for the PSS installed in generator G_5 is

$\omega_5 - \sum_{k=1,3,6-9} \omega_k$ and the matrix K is correspondence to:

$$\mathbf{K} = [-1 \ -1 \ -1 \ 0 \ 1 \ -1 \ -1 \ -1 \ -1 \ 0] \quad (23)$$

C.2. Second scenario

The main focus of this section is the use of proposed approach (GMDC-based, two-stage method) to design damping controllers, specifically to tune parameters of POD used in the IPFC-POD device. The main steps of this method are:

- Step 1: Using an optimization algorithm to regulate PSSs equipped to suppress, local mode oscillations.
- Step 2: Using the GMDC-based method for designing an SDC that is considered for IPFC-POD to more suppression of inter-area mode oscillations.

In the first step of design, the objective function of F_1 is solved through GRSA to provide PSS parameters that are equipped in generators $\{G_1$ to G_5 and G_7 to $G_9\}$. In the second step, the POD parameters are determined by GMDC.

It should be noted that the PSS feedback input signal, which is installed on G_5 , is calculated as in the first scenario. The designed POD contains a filter which follows the inter-area mode. The transfer function of that is constructed based on the following equations:

$$G_R(s) = 10 \frac{10s}{1+10s} \left(\frac{1+0.0781s}{1+0.0236s} \right)^2 \quad (24)$$

$$G_{POD}(s) = \frac{1.0099s}{s^2 + 1.0099s + 9.1795} G_R(s) \quad (25)$$

Table 3 shows PSS parameters tuned with GRSA and also POD parameters searched based on GMDC method, respectively.

To illustrate the effectiveness of the designed controller, simulation has been performed to evaluate the response of the test system to the specified disturbance as follows:

- A three-phase fault of the short circuit type at the end-bus of the tie-line 26-29 at $t = 1$ s. It is assumed that the fault is cleared after 100 ms, by tripping the faulty line.

D. Eigenvalue Analysis and Simulation Results

This subsection presents probabilistic results of critical modes in the two reviewed scenarios. The classified results of eigenvalue analysis are shown in Table 4. The main purpose of this subsection is to indicate the effectiveness of the proposed technique (second scenario) to more suppress of inter-area modes. In both scenarios, local modes have adequate damping and analyses of inter-area mode damping has an active area of research. Also, local mode's damping is approximately steady on average and do not vary significantly from the first to the second scenario.

In Table 4, the stability of mode-9 (inter-area mode) in the scenario 1 is slightly inadequate ($\alpha_9^* = 10.802$, $\xi_9^* = 1.235$) and should be enhanced. By applying the intended method (second scenario), all the electro-mechanical modes are well damped and high reliable indices have been achieved ($\alpha_9^* = 13.703$, $\xi_9^* = 5.332$). The comparison of the best results of both scenarios, superiority of obtained results in the second scenario has been proved. In order to more investigation of dynamic stability of the test system, placement of the nine electromechanical modes are drawn graphically in complex s-plane in Figure 7. As is obvious in this figure, extracted eigenvalues of both scenarios can be bounded in the fan-shaped region with the apex at the origin coordinates charts.

Nevertheless, access to the higher value of damping ratio in the second scenario, especially for inter-area mode is clearly visible.

The analysis of Figure 8 depicts that as expected, the generator responses of the second scenario which involve in the local modes are most like to the first scenario.

According to the sensitivity analysis presented in the second section, the concerned inter-area mode (9th mode) has relatively more effect on the rotor angle deviation of $\Delta\delta_{25}$.

Hence, as the proposed approach of the paper is specifically relate to the inter-area mode's stability improvement, accessing to the lower values of the oscillation frequency and settling time in the second scenario for $\Delta\delta_{25}$ can be reasonable, which is obtained.

In order to do a clear investigation and a complementary study in the system response for different type of scenarios, two of common performance indices (PI) which are respectively related to the settling time and overshoot in speed response (ISTSE, and ISE), are described as Eqs. (26) and (27), where ISTSE and ISE denote 'Integral of Squared Time-Square Error' and 'Integral Square Error', respectively.

$$ISTSE(PI_1) = \sum_{i=1}^{n_m} \int_{t=0}^{t=t_{sim}} (t\Delta\omega_i(t))^2 dt \quad (26)$$

$$ISE(PI_2) = \sum_{i=1}^{n_m} \int_{t=0}^{t=t_{sim}} (\Delta\omega_i(t))^2 dt \quad (27)$$

The results of extracted performance indices which attributed to the defined scenarios are listed in Table 5. In order to more analyses of presented scenarios, the worst four cases of 12, 26, 38 and 43 which have the lowest margin of stability are selected (Correspondence to C.1, C.2, C.3 and C.4 in Table 5.

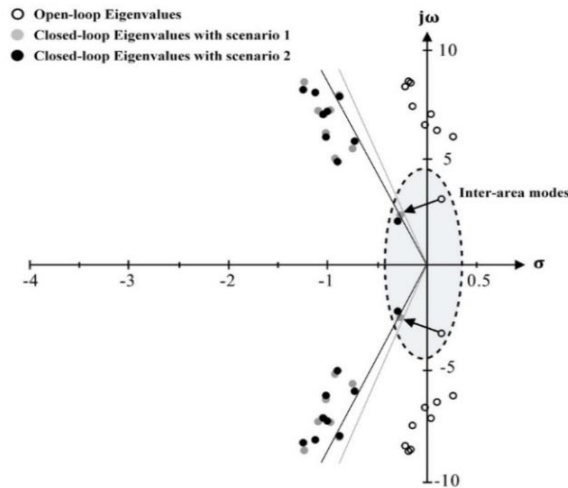


Fig. 7: Dominant open-loop and closed-loop eigenvalues of the test system by considering two scenarios.

Table 3: Gains and time constants of the pss controllers adjusted by different methods

Device	Scenario 1			Scenario 2		
	K^{pss}/K^{pod} [p.u.]	T_1^{pss}/T_1^{pod} [s]	T_2^{pss}/T_2^{pod} [s]	K^{pss}/K^{pod} [p.u.]	T_1^{pss}/T_1^{pod} [s]	T_2^{pss}/T_2^{pod} [s]
PSS G ₁	7.2812	1.0250	0.0691	9.1349	1.2025	0.0897
PSS G ₂	7.4586	0.7205	0.0299	9.1763	0.7615	0.0310
PSS G ₃	7.3126	0.6132	0.0306	7.0251	0.5002	0.0211
PSS G ₄	8.6259	0.5208	0.0728	9.1375	0.6258	0.0516
PSS G ₅	7.0336	0.5214	0.0701	7.5423	0.6417	0.0912
PSS G ₇	1.9948	0.4216	0.0658	8.7256	0.5610	0.0543
PSS G ₈	8.1622	0.6705	0.0413	7.5418	0.8211	0.0350
PSS G ₉	6.4896	0.2925	0.0763	9.2462	0.2925	0.0763
IPFC-POD	7.8236	0.3347	0.0823	10	0.0781	0.0236

Table 4: Result of concerned closed-loop modes by different methodes

No.	Scenario 1							Scenario 2						
	$\bar{\alpha}$	$\bar{\beta}$	σ_α	α^*	$\bar{\xi}$	σ_ξ	ξ^*	$\bar{\alpha}$	$\bar{\beta}$	σ_α	α^*	$\bar{\xi}$	σ_ξ	ξ^*
1	-1.219	8.312	0.0093	129.02	0.145	0.0008	58.035	-1.229	7.963	0.009	128.036	0.152	0.0009	60.202
2	-1.079	7.014	0.0096	125.49	0.152	0.0011	49.369	-1.108	7.835	0.009	115.326	0.140	0.0010	38.265
3	-0.868	7.723	0.0078	123.56	0.111	0.0005	22.637	-0.863	7.654	0.008	102.021	0.112	0.0004	28.215
4	-0.956	7.040	0.1858	5.124	0.134	0.0061	5.674	-0.987	6.980	0.160	6.172	0.140	0.0066	6.109
5	-1.001	6.012	0.1869	6.013	0.164	0.0128	5.026	-1.000	5.831	0.131	7.621	0.169	0.0111	6.240
6	-1.035	6.846	0.0964	10.228	0.149	0.0088	5.614	-1.027	6.851	0.100	10.228	0.148	0.0097	4.984
7	-0.732	5.305	0.0470	14.112	0.136	0.0047	7.865	-0.711	5.642	0.065	10.915	0.125	0.0036	6.974
8	-0.909	4.865	0.0652	15.063	0.183	0.0051	16.468	-0.884	4.716	0.071	12.361	0.184	0.0067	12.580
9	-0.251	2.311	0.0220	10.802	0.108	0.0067	1.235	-0.278	2.031	0.020	13.703	0.135	0.0067	5.332

It should be mentioned that achieve to the lower values of these indices caused to develop the range of dynamic stability of the power system. The superiority of the designed powerful device can be clear from the comparison between both scenarios in each state of operating condition.

Table 5: Performance indices of the test system in different conditions

Scenario	S.1				S.2			
	C.1	C.2	C.3	C.4	C.1v	C.2	C.3	C.4
Case no.								
PI_1	1.25	1.23	1.22	1.231	1.17	1.12	1.15	1.10
PI_2	2.82	2.67	2.80	2.732	2.45	2.19	2.40	2.32

Table A.1: Strategy Parameters of Optimization Algorithm (GRSA)

Strategy parameter	Default value
h (Search subspace size)	$10 \times d$
S (Number of search subspaces)	$[d/3]$
S_s (Search space size)	$S \times h$
t_{max} (Maximum number of iterations)	$10 \times n$
GM_{max} (Maximum of geometry coefficient)	1
GM_{min} (Minimum of geometry coefficient)	0
GM_1 (Geometry coefficient)	0.01
GM_2 (Geometry coefficient)	0.99

Conclusion

The main goal of this paper was about the introduction of a non-typical IPFC-POD design methodology. The small-signal stability assessment of the test system was adopted from a developed dynamic model of power system accompanied by an IPFC device.

The organization of the paper was based on two scenarios. In the first scenario, the results of the analysis were reported according to the existing method, and in the second scenario, the comparison with the proposed method was made in detail. In general, the specific purpose of this paper was to enhance the dynamic stability of concerned inter-area modes. The proposed method, especially using GRSA, offers better stability characteristics than the results of the first scenario. A numerical analysis which was carried out based on the PSIs over a large set of operating conditions was take place, and then the result was verified through the time-domain simulation.

Appendix

The parameters of the implicit optimization algorithm that must be provided prior to the optimization process are presented in Table A.1. Also, the information required in the paper to evaluate the proposed method are listed in Table A.2.

Table A.2: Requirement data

Parameter	Symbol	Value
Fixed center frequency of filter (rad/s)	ω_0	3.0298
Quality factor of the filter	Q	3
Simulation time (sec)	t_{sim}	14
Number of series loads	n_l	50

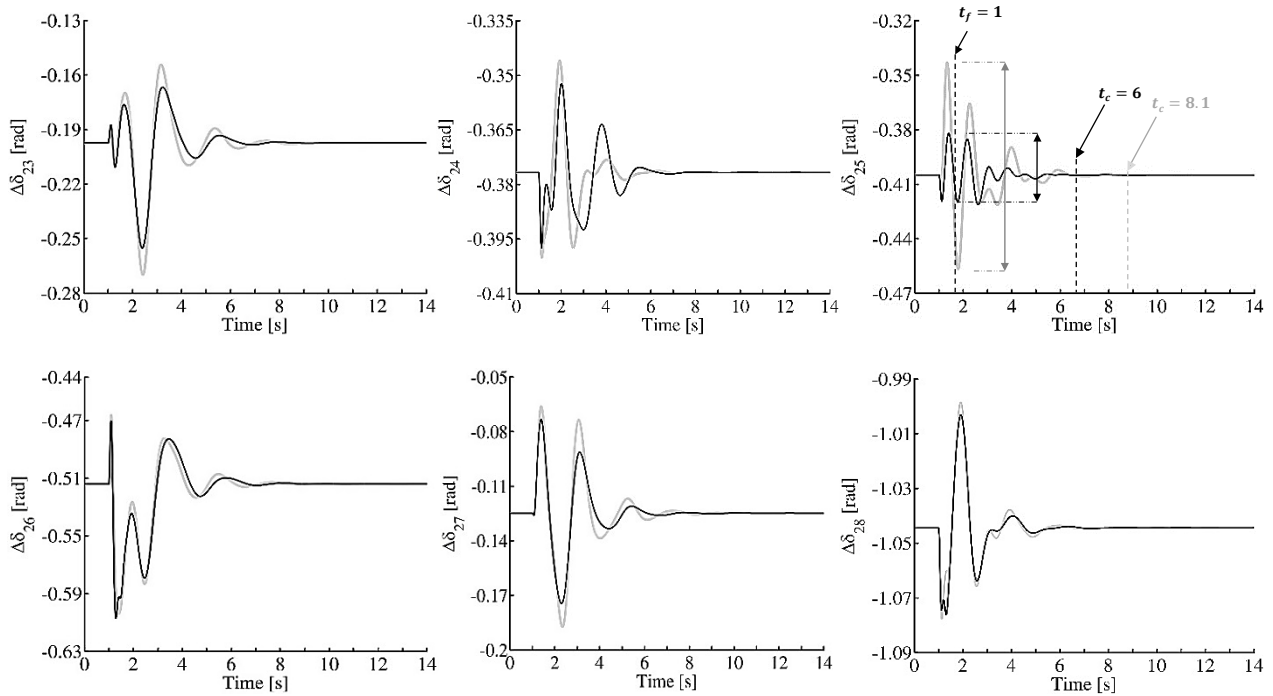


Fig. 8: Rotor angle deviation of the different generators.

Results and Discussion

It is obvious that increasing the small-signal stability with a predetermined POD controller can provide a situation that exceeds the positive effect of additional damping and reduces the detrimental effect of the weak

inter-area mode's damping in the overall dynamic stability.

Author Contributions

B. Ehsanmaleki has found a new method for redesign of POD which will be connected to facts devices. H. Beiranvand also has presented new specific

strategy for co-working of POD with all powerful facts devices. B. Ehsanmaleki and P.Naderi interpreted the results and wrote the manuscript.

Conflict of Interest

The author declares that there is no conflict of interests regarding the publication of this manuscript. In addition, the ethical issues, including plagiarism, informed consent, misconduct, data fabrication and/or falsification, double publication and/or submission, and redundancy have been completely observed by the authors.

Abbreviations

A, B, C, D	Constant matrixes of the state space equation
C_{dc}	Capacitance of the DC-link capacitor
E_{fdi}	D-axes component of the field voltage of the i^{th} excitation system (V)
E'_q	Q-axes component of the generator's internal voltage (V)
$G_R(s)$	Transfer function of the RPSS
$G_{POD}(s)$	Transfer function of the POD
h_k	Parameter of the voltage magnitude vector
I_{IP}	Current matrix of the IPFC device
I_{new}	New form of the system's current matrix
I_{sei}	Seri current vector of the i^{th} transformer (A)
I_{seid}	D-axes component of current vector of the i^{th} series transformer (A)
I_{seiq}	Q-axes component of current vector of the i^{th} series transformer (A)
I_{BUS}	Current matrix of the system
I_S	Current matrix of the source
I_G	Current matrix of the generator
K_{Ai}	Gain of the i^{th} excitation system
K	Output signal combination vector
K_i^{PSS}	Optimal value of the i^{th} PSS gain
m_i	Phase modulation index of the each VSCs
n	Numbers of the state variables
n_m	Number of machines in the test system
n_q	Number of eigenvalues in the test system
l_k	Controller parameter of the voltage magnitude vector
r_{CST}	Resistant of the coupler series transformers
t_{sim}	Simulation time interval
T_{ji}	Optimal value of the j^{th} time constants of the i^{th} PSS (sec)
$T_i^{PSS/POD}$	Optimal value of the i^{th} time constants of the PSS/POD (sec)
T_{Ai}	Time constant of the i^{th} excitation system (sec)
P_{IPFC}	Summation of the active power of the VSCs (W)
P_{Mk}	Mechanical power of the k^{th} tie-line
q	Subscript index of eigenvalue of the test system
U	Vector of the input variable

V_{PSSi}	Output voltage of the i^{th} PSS (V)
V_{ti}	Terminal voltage of the i^{th} generator (V)
V_{refi}	Reference voltage of the i^{th} generator (V)
V_{inj_i}	Injection voltage vector of the i^{th} series transformer (V)
$V_{inj_{id}}$	D-axes component of injection-voltage vector of the i^{th} series transformer (V)
$V_{inj_{iq}}$	Q-axes component of injection-voltage vector of the i^{th} series transformer (V)
V_{sei}	Voltage vector of the i^{th} series transformer (V)
V_{seid}	D-axes component of voltage vector of the i^{th} series transformer (V)
V_{seiq}	Q-axes component of voltage vector of the i^{th} series transformer (V)
V_{dc}	Voltage vector of the DC-link capacitor (V)
V_{BUS}	Voltage matrix of the system
V_d	D-axes component of the voltage vector (V)
V_q	Q-axes component of the voltage vector (V)
V_{new}	New form of the system's voltage matrix
V_S	Voltage matrix of the source
V_G	Voltage matrix of the generator
V_{IP}	Voltage matrix of the IPFC device
x_{t1}	First side reactance of the series transformer
x_{t2}	Second side reactance of the series transformer
x'_d	D-axes component of the transformer transient reactance
x_q	Q-axes component of the transformer reactance
X	Vector of the state variable
y_i	WAPSS feedback signal to damp the i^{th} mode
y	Subscript index of the system's operating condition
Y_{BUS}	Admittance matrix of the system
Y_{new}	New form of the system's admittance matrix
σ_{α_k}	Standard deviation of the k^{th} eigenvalue's real part
$\bar{\alpha}_k$	Average value of the k^{th} eigenvalue's real part
$\bar{\beta}_k$	Average value of the k^{th} eigenvalue's imag part
α'_k	Extended damping coefficient of the k^{th} eigenvalue
ξ'_k	Extended damping ratio of the k^{th} eigenvalue
$\bar{\xi}_k$	Average value of the k^{th} eigenvalue's damping ratio
σ_{ξ_k}	Standard deviation of the k^{th} eigenvalue's damping ratio
ξ_C	Desired value of the damping ratio
α_k^*	Standardized expectation of the k^{th} eigenvalue
ξ_k^*	Standardized damping ratio of the k^{th} eigenvalue

γ_k	Phase angle of the voltage magnitude vector (rad)
ψ_k	Controller parameter of the voltage angle vector (rad)
φ_i	Phase modulation index of the each VSCs (rad)
λ_i	Modes of the eigenvalue matrix
δ	Rotor angle of the rotor (rad)
ω_i	Angular speed of the i^{th} machine (rad/s)
ξ_q	Damping ratio of the q^{th} eigenvalue
ξ_0	Expected value of damping ratio

References

[1] A. F. Bati "Optimal interaction between PSS and FACTS devices in damping power systems oscillations: Part II," in Proc. 2010 IEEE International Energy Conference: 452-457, 2010.

[2] N. Rezaei, M. Kalantar, H. A. Shayanfar, Y. Alipouri, A. Safari, "Optimal IPFC signal selection and damping controller design using a novel current injection model in a multi-machine power system," International Journal of Electrical Power and Energy Systems, 44(1): 461-70, 2013.

[3] A. Kumar, "Power system stabilizers design for multi-machine power systems using local measurements," IEEE Transactions on Power Systems, 31(3): 2163-2171, 2016.

[4] M. R. Shakarami, I. F. Davoudkhani, "Wide-area power system stabilizer design based on grey wolf optimization algorithm considering the time delay," Electric Power Systems Research, 133: 149-159, 2016.

[5] B. Ehsan-Maleki, P. Naderi, H. Beiranvand, "A novel 2-stage WAPSS design method to improve inter-area mode damping in power systems," International Transactions on Electrical Energy Systems, 2018 Mar; 28(3): e2503, 2018.

[6] D. D. Simfukwe, B. C. Pal, R. A. Jabr, N. Martins, "Robust and low-order design of flexible ac transmission systems and power system stabilisers for oscillation damping," IET generation, transmission & distribution, 6(5): 445-452, 2012.

[7] E. Gholipour, G. H. Isazadeh, "Design of a new adaptive optimal wide area IPFC damping controller in Iran transmission network," International Journal of Electrical Power & Energy Systems, 53: 529-539, 2013.

[8] M. A. Furini, A. L. Pereira, P. B. Araujo, "Pole placement by coordinated tuning of power system stabilizers and FACTS-POD stabilizers," International Journal of Electrical Power & Energy Systems, 33(3): 615-622, 2011.

[9] S. Bhowmick, B. Das, N. Kumar, "An advanced IPFC model to reuse Newton power flow codes," IEEE Transactions on Power Systems, 24(2): 525-532, 2009.

[10] J. Guo, M. L. Crow, J. Sarangapani, "An improved UPFC control for oscillation damping," IEEE Transactions on Power Systems, 24(1): 288-296, 2009.

[11] X. Y. Bian, C. T. Tse, J. F. Zhang, K.W. Wang, "Coordinated design of probabilistic PSS and SVC damping controllers," International Journal of Electrical Power & Energy Systems, 33(3): 445-452, 2011.

[12] H. Shayeghi, A. Safari, H. A. Shayanfar, "PSS and TCSC damping controller coordinated design using PSO in multi-machine power system," Energy Conversion and Management, 51(12): 2930-2937, 2010.

[13] R. Visakhian, R. Rahul, A. A. Kurian, "Comparative study of PSS and FACTS-POD for power system performance enhancement," in Proc. 2015 International Conference on Power, Instrumentation, Control and Computing (PICC): 1-6, 2015.

[14] C. R. Makkar, L. Dewan, "Simultaneous coordination of Power System Stabilizer and UPFC for improving dynamic stability of

multimachine system," in Proc. 2014 IEEE 6th India International Conference on Power Electronics (IICPE): 1-4, 2014.

[15] M. Khaleghi, M. M. Farsangi, H. Nezamabadi-Pour, K. Y. Lee, "Pareto-optimal design of damping controllers using modified artificial immune algorithm," IEEE Transactions on Systems, Man, and Cybernetics, Part C, 41(2): 240-250, 2011.

[16] H. Beiranvand, E. Rokrok, "General relativity search algorithm: a global optimization approach," International Journal of Computational Intelligence and Applications, 14(3), 2015.

[17] M. Khederzadeh, A. Ghorbani, "Impact of VSC-based multilane FACTS controllers on distance protection of transmission lines," IEEE transactions on Power delivery, 27(1): 32-39, 2012.

[18] A. Kazemi, E. Karimi, "The effect of interline power flow controller (IPFC) on damping interarea oscillations in the interconnected power systems," in Proc. The 41st International Universities Power Engineering Conference: 769-773, 2006.

[19] A. M. Parimi, I. Elamvazuthi, N. Saad, "Interline power flow controller application for low frequency oscillations damping," WSEAS Transactions on Systems, 9(5): 511-527, 2010.

[20] P. W. Sauer, M. A. Pai, Power System Dynamics and Stability, Urbana, 1998.

[21] S. K. Wang, "A novel objective function and algorithm for optimal PSS parameter design in a multi-machine power system," IEEE Transactions on Power Systems, 28(1): 522-531, 2013.

[22] J. Zhang, C. Y. Chung, Y. Han, "A novel modal decomposition control and its application to PSS design for damping interarea oscillations in power systems," IEEE Transactions on Power Systems, 27(4), 2015-2025, 2012.

[23] Y. Yuan, Y. Sun, and L. Cheng, "Determination of wide-area PSS locations and feedback signals using improved residue matrices," in Proc. 2008 IEEE Asia Pacific Conference on Circuits and Systems): 762-765, 2008.

[24] S. Aboreshaid, R. Billinton, M. Fotuhi-Firuzabad, "Probabilistic transient stability studies using the method of bisection [power systems]," IEEE Transactions on Power Systems, 11(4): 1990-1995, 1996.

[25] C. T. Tse, K. W. Wang, C. Y. Chung, K. M. Tsang, "Robust PSS design by probabilistic eigenvalue sensitivity analysis," Electric Power Systems Research, 59(1): 47-54, 2001.

Biographies



Behzad Ehsan maleki was born on 6st May 1991 in Tehran, Iran. He obtained scholarship from the Ministry of Education, Iran in 2009 to peruse the BSc./B.Tech degree in Electrical Engineering. He received BSc./B.Tech and MSc./M.Tech degree in Electrical Engineering from Lorestan University and Shaheed Rajae Teacher Training University in 2013 and 2016, respectively. His current research interests are Power System Stability and Flexible Alternating Current Transmission System (FACTS) devices.



Hamzeh Beiranvand was born on 21st March 1989 in Khorramabad, Iran. He obtained scholarship from the Ministry of Education, Iran in 2007 to peruse the BSc./B.Tech degree in Electrical Engineering. He received BSc./B.Tech and MSc./M.Tech degree in Electrical Engineering from Lorestan University in 2011 and 2014, respectively. He started his Ph.D. in the year 2015 at Lorestan University and currently working on Solid-State Transformers (SSTs) in collaboration with chair of power electronics, Christian-Albrechts-Universität zü Kiel, Germany. His current research interests are Power Electronic Converters, Modular Multi-level Converters (MMCs), and SSTs.

Copyrights

©2020 The author(s). This is an open access article distributed under the terms of the Creative Commons Attribution (CC BY 4.0), which permits unrestricted use, distribution, and reproduction in any medium, as long as the original authors and source are cited. No permission is required from the authors or the publishers.



How to cite this paper:

B. Ehsan Maleki, H. Beiranvand, "A Novel Method of FACTS-POD Design to More Enhancement of Inter-Area Mode Damping in A Multi-Machine Power System," Journal of Electrical and Computer Engineering Innovations, 6(1): 97-109, 2018.

DOI: 10.22061/JECEI.2018.1102

URL: http://jecei.sru.ac.ir/article_1102.html

